*Final Draft*
**of the original manuscript:**

Brocks, W.; Anuschewski, P.; Scheider, I.
**Ductile Tearing Resistance of Metal Sheets**
In: Engineering Failure Analysis (2009) Elsevier

DOI: 10.1016/j.engfailanal.2009.03.021

# Ductile Tearing Resistance of Metal Sheets

Wolfgang Brocks[1,a], Paul Anuschewski[1] and Ingo Scheider[1,b]

[1] Materials Mechanics, Institute of Materials Research, GKSS Research Centre, D-21502 Geesthacht, Germany

[a] wolfgang.brocks@gkss.de, [b] ingo.scheider@gkss.de

**Keywords:** Ductile tearing, R-curves, *J*-integral, dissipation rate, cracked panel, sheet metal.

**Abstract**. The concept of R-curves has been adopted to characterise stable crack extension and predict residual strength of thin-walled structures particularly in the aircraft industry. The present contribution uses results of FE simulations of crack extension in panels by the cohesive model to validate analytical procedures for determining *J*-integral values at large crack extension from measurable quantities, namely the force vs. displacement records. The numerically determined *J*-integral is taken as the benchmark for the outcome of the analytical formulas. The geometry dependence of *J* and CTOD based R-curves is investigated and alternative concepts like CTOA and dissipation rate at crack extension are discussed.

## Nomenclature

| | |
|---|---|
| $A$ | total crack area, $A = Ba$ for C(T), $A = 2Ba$ for M(T) |
| $a$ | current crack length of C(T), half crack length of M(T) |
| $a_0$ | initial crack length |
| $a_{\mathrm{eff}}$ | "effective" crack length according to ASTM E 561 |
| $a_{(i)}$ | crack length at load step ($i$) |
| $b$ | length of crack ligament, $b = W - a$ |
| $B$ | specimen thickness |
| $C$ | compliance, $C = V/F$ |
| $\Delta a$ | crack extension at one crack tip with respect to initial crack length, $\Delta a = a - a_0$ |
| $\Delta a_{(\mathrm{i})}$ | crack extension during a loading increment, $\Delta a_{(i)} = a_{(i)} - a_{(i-1)}$ |
| $\Delta f_{(i)}$ | increment of any quantity, $f$, $\Delta f_{(i)} = f_{(i)} - f_{(i-1)}$ |
| $\delta_{\mathrm{n}}$ | material separation in the process zone, $\delta_{\mathrm{n}} = [u_{\mathrm{n}}] = u_{\mathrm{n}}^{+} - u_{\mathrm{n}}^{-}$ |
| $E$ | Young's modulus |
| $F$ | force |
| $\Gamma_{\mathrm{c}}$ | separation energy (mode I), $\Gamma_{\mathrm{c}} = \int_0^{\delta_{\mathrm{c}}} \sigma_{\mathrm{n}} \, \mathrm{d}\delta_{\mathrm{n}}$ |
| $J$ | *J*-integral |
| $K$ | stress intensity factor for mode I |
| $r_{\mathrm{pl}}$ | radius of plastic zone at the crack tip according to Irwin |

$R^{dis}$ dissipation rate

$R_Y$ yield strength

$R_\infty^{dis}$ crack-propagation energy rate for stationary crack extension

$\sigma_c$ cohesive strength

$\sigma_n$ cohesive (normal) stresses in the process zone

$U$ strain energy

$V_L$ load point displacement

$V_{LL}$ load line displacement of C(T)

$V_M$ crack (mouth) opening displacement (CMOD) in the symmetry line of M(T)

$W$ specimen width of C(T), half specimen width of M(T)

$W^{ex}$ work of external forces

sub- and superscripts

dis dissipation, dissipated

eff effective

el elastic, elastic part

ex external

L load point

LL load line

M crack mouth

pl plastic, plastic part

R resistance

sep separation

($i$) load step ($i$)

## Introduction

The familiar concept of $J_R$-curves originally established for thick-walled components under plane-strain conditions has also been adopted to characterise stable crack extension and predict residual strength of thin-walled components under plane-stress conditions, particularly in the aircraft industry. It requires other specimen types, primarily large cracked tensile panels allowing for pronounced ductile crack extension prior to failure. The respective test procedures and standards are not as well founded as those for plane-strain specimens. ASTM E 1820 [1] does not include M(T) specimens at all, and ASTM E 561 [2] yields R-curves in terms of the stress intensity factor as a function of the "effective" crack length. The new ASTM E 2472 [3] addresses the

determination of resistance to stable crack extension under low-constraint conditions in terms of crack-tip opening displacement (CTOD) and crack-tip opening angle (CTOA).

Though the knowledge about the evaluation of $J_R$-curves from force-displacement records is quite old, namely more than 30 years, the formulas extracted from the literature are still controversial, which impedes any sound discussion on the validity of R-curves, as experimental investigations on this matter suffer from inconsistent data. The present contribution uses results of FE simulations of crack extension in panels by the cohesive model to validate analytical procedures for determining *J*-integral values at large crack extensions from measurable quantities. The numerically calculated *J*-integral is taken as the benchmark for the outcome of the analytical formulas. As no general discussion on the *significance* of R-curves for characterising ductile crack extension is intended, no respective "*validity conditions*" have to be considered. However assuring that at least a *correct J*-value has been determined is a necessary prerequisite for discussing the problem of *transferability* of $J_R$-curves, which is sometimes ignored in experimental investigations. The term *validity* should be avoided anyway, as it is ambiguously used for both *accuracy* of the evaluation formula and *significance* of *J* as a parameter controlling crack extension.

## Basic Equations

### The *J*-Integral as Energy Release Rate.

The basic idea of determining *J* from an experimental force-displacement record is more than 30 years old. It utilises the nature of *J* being an energy release rate in the deformation theory of plasticity [4], [5],

$$J = -\left(\frac{\partial U}{\partial A}\right)_{V_\mathrm{L}} = -\int_0^V \left(\frac{\partial F}{\partial A}\right)_{V_\mathrm{L}} dV = \left(\frac{\partial U}{\partial A}\right)_F = \int_0^F \left(\frac{\partial V_\mathrm{L}}{\partial A}\right)_F dF \,. \tag{1}$$

For a panel shaped specimen of thickness *B* with a through-crack and a straight crack front we have $\Delta A = B\Delta a = -B\Delta b$ for each crack tip, where $b = W - a$ is the ligament length, i.e. $\partial/\partial A = \partial/B\partial a$ for C(T), SE(T), SE(B) and $\partial/\partial A = \partial/2B\partial a$ for M(T) and DE(T).

The load-point displacement, $V_\mathrm{L}$, is split into an elastic (linear, reversible) and a plastic (nonlinear, permanent) part, $V_\mathrm{L} = V_\mathrm{L}^\mathrm{el} + V_\mathrm{L}^\mathrm{pl}$, and so is the mechanical work or deformation energy and, hence, the *J*-integral,

$$U = \int_0^V F\,dV = \int_0^{V_\mathrm{L}^\mathrm{el}} F\,dV_\mathrm{L}^\mathrm{el} + \int_0^{V_\mathrm{L}^\mathrm{pl}} F\,dV^\mathrm{pl} = \tfrac{1}{2} F V_\mathrm{L}^\mathrm{el} + \int_0^{v_\mathrm{L}^\mathrm{pl}} F\,dV_\mathrm{L}^\mathrm{pl} = U^\mathrm{el} + U^\mathrm{pl} \,. \tag{2}$$

$$J = J^\mathrm{el} + J^\mathrm{pl}. \tag{3}$$

Applying this separation in elastic and plastic fractions, eq. (1) holds likewise for $J^\mathrm{pl}$, $U^\mathrm{pl}$, and $V^\mathrm{pl}$. The elastic part is calculated from the mode I stress intensity factor, assuming plane stress conditions in metal sheets

$$J^{\mathrm{el}} = \frac{K^2}{E} \qquad \text{with} \qquad K_{\mathrm{I}} = \sigma_\infty \sqrt{\pi a}\, Y\left(a/W\right). \tag{4}$$

**The $K_{\mathrm{eff}}$ Concept.**

ASTM E 561 [2] regulates the determination of $K_{\mathrm{R}}$-curves, i.e. $K_{\mathrm{eff}} = K\left(a_{\mathrm{eff}}\right)$, as crack growth resistance, "so long as specimens are of sufficient size to remain predominantly elastic throughout the duration of the test". What this statement actually means, will be discussed below. Two options of determining $a_{\mathrm{eff}}$ are proposed. Under small scale yielding conditions, the stress field is dominated by an "effective" stress intensity factor, which - according to Irwin - results from a plastic zone correction of the physical crack length by the radius of the plastic zone,

$$a_{\mathrm{eff}} = a + r_{\mathrm{pl}} = a_0 + \Delta a + r_{\mathrm{pl}} = a_0 + \Delta a_{\mathrm{eff}} \qquad \text{with} \qquad r_{\mathrm{pl}} = \frac{1}{2\pi}\left(\frac{K}{R_{\mathrm{Y}}}\right)^2, \tag{5}$$

assuming plane stress, again. $K$ can be modified once by $a_{\mathrm{eff}}$ according to eq. (5) to yield $K_{\mathrm{eff}}$ or iteratively, as $a_{\mathrm{eff}}$ depends on $K$. Alternatively, $a_{\mathrm{eff}}$ can be calculated from the compliance of the specimen, regarding the elastic-plastic deformation of the specimen with crack length $a$ as an elastic deformation of a (fictitious) specimen with crack length $a_{\mathrm{eff}}$ ,

$$V = V^{\mathrm{el}} + V^{\mathrm{pl}} = C\left(a\right)F + V^{\mathrm{pl}} = C\left(a_{\mathrm{eff}}\right)F \ . \tag{6}$$

The compliance is determined experimentally or from analytical formulas. For comparison with other R-curve formulas, $K_{\mathrm{eff}}$ will be converted to $J$ according to eq. (4).

## $J_{\mathrm{R}}$-Curves for Cracked Metal Sheets

### C(T) Specimens

ASTM E 1820 [1] is the standard test method for measurement of fracture toughness on bend-type specimens. The basic assumption is that a specimen, which has undergone crack extension, has the same value of $J_{(i)}$ as a postulated non-linear elastic specimen at the same load, $F_{(i)}$, displacement, $v_{(i)}$, and final crack length, $a_{(i)}$, which was not subject to crack extension. The problem reduces to constructing a force-displacement curve for such a specimen. Though this standard is particularly designated to thick (plane strain) specimens, the evaluation formulas do not explicitly contain any restriction with respect to the thickness of the test piece.

The elastic part of $J$ is calculated according to eq. (4), where the geometry function $Y\left(a/W\right)$ is provided in the standards [1], [2]. Starting from the value at crack initiation, $J^{\mathrm{pl}} = \eta U^{\mathrm{pl}} \big/ B b_0$, further values are calculated stepwise for crack extension increments, $\Delta a_{(i)} = a_{(i)} - a_{(i-1)}$,

$$J^{\mathrm{pl}}_{(i)} = J^{\mathrm{pl}}\left(a_{(i)}\right) = J^{\mathrm{pl}}_{(i-1)} + \Delta J^{\mathrm{pl}}_{(i)} = \left(J^{\mathrm{pl}}_{(i-1)} + \frac{\eta_{(i-1)}}{b_{(i-1)}}\frac{\Delta U^{\mathrm{pl}}_{(i)}}{B}\right)\left(1 - \gamma_{(i-1)}\frac{\Delta a_{(i)}}{b_{(i-1)}}\right) \ , \tag{7}$$

where $\eta$ and $\gamma$ are the well-known geometry functions for C(T) specimens and $b = W - a$. The increment of plastic work is determined from the area under the (experimental) load-displacement curve,

$$\Delta U^{\mathrm{pl}}_{(i)} = U^{\mathrm{pl}}_{(i)} - U^{\mathrm{pl}}_{(i-1)} = \int_{V^{\mathrm{pl}}_{\mathrm{LL}(i-1)}}^{V^{\mathrm{pl}}_{\mathrm{LL}(i)}} F \, dV^{\mathrm{pl}}_{\mathrm{LL}} = \tfrac{1}{2}\left(F_{(i)} + F_{(i-1)}\right) \Delta V^{\mathrm{pl}}_{\mathrm{LL}(i)} \quad , \tag{8}$$

where $V_{\mathrm{LL}}$ is the load-line displacement, whose plastic part is calculated by means of the elastic compliance, $V^{\mathrm{pl}}_{\mathrm{LL}} = V_{\mathrm{LL}} - C_{\mathrm{LL}}(a)F$ [1].

**M(T) Specimens.**

There is no standard like ASTM E 1820 [1] for tensile-type fracture specimens. Several formulas have been derived in the literature but never been standardised. The elastic part results from *K*, again, where commonly the "secans formula" of Feddersen [6] for the geometry function is applied

$$Y\left(\frac{a}{W}\right) = \sqrt{\sec\left(\frac{\pi a}{2W}\right)} = \frac{1}{\sqrt{\cos\left(\pi a / 2W\right)}} . \tag{9}$$

ASTM E 561 [2] provides an alternative expression, which appeared to be improper for $(a/W) > 0.6$, however.

Based on eq. (1), Rice et al. [5] have derived the formula

$$J^{\mathrm{pl}} = \frac{1}{bB}\left[\int_0^{V^{\mathrm{pl}}_{\mathrm{L}}} F \, dV^{\mathrm{pl}}_{\mathrm{L}} - \tfrac{1}{2} F V^{\mathrm{pl}}_{\mathrm{L}}\right] = \frac{1}{bB}\left(U^{\mathrm{pl}} - \tfrac{1}{2} F V^{\mathrm{pl}}_{\mathrm{L}}\right) = \frac{U^{*}}{bB} , \tag{10}$$

for an M(T) specimen with constant crack length. This equation can be extended to crack growth by the assumption explained for the C(T), above. It results in

$$J^{\mathrm{pl}}_{(i)} = J^{\mathrm{pl}}_{(i-1)} \frac{b_{(i)}}{b_{(i-1)}} + \frac{F_{(i-1)} V^{\mathrm{pl}}_{\mathrm{L}(i)} - F_{(i)} V^{\mathrm{pl}}_{\mathrm{L}(i-1)}}{2 B b_{(i-1)}} . \tag{11}$$

Local plastic deformations at the point of applied load, which are not relevant for *J*, are disregarded. As long as no plastic deformations occur in the symmetry line between the load points and the measuring points of crack opening (CMOD),

$$V^{\mathrm{pl}}_{\mathrm{L}} = V_{\mathrm{L}} - V^{\mathrm{el}}_{\mathrm{L}} = V^{\mathrm{pl}}_{\mathrm{M}} = V_{\mathrm{M}} - V^{\mathrm{el}}_{\mathrm{M}} = V^{\mathrm{pl}} . \tag{12}$$

This does not hold for the total displacement, of course. The elastic parts, $V^{\mathrm{el}}_{\mathrm{L}}$ and $V^{\mathrm{el}}_{\mathrm{M}}$, can be calculated from the respective compliances, $C_{\mathrm{L}}$ and $C_{\mathrm{M}}$ [2], [7], [8].

Garwood et al. [9] proposed a procedure to calculate the total $J$ from the load-displacement curve. It yields

$$J_{(i)} = J_{(i-1)} \frac{b_{(i)}}{b_{(i-1)}} + \frac{F_{(i-1)} v_{\mathrm{L}(i)} - F_{(i)} v_{\mathrm{L}(i-1)}}{2Bb_{(i-1)}} + \frac{K_{(i)}^2 b_{(i)} - K_{(i-1)}^2 b_{(i-1)}}{Eb_{(i-1)}}, \tag{13}$$

which is slightly different from the total $J$ calculated according to eq (11) and adding the elastic part from eq. (4).

Hellmann and Schwalbe [10] provide a formula with reference to Garwood et al. [9] but have apparently missed that the increment of crack surface in an M(T) specimen is $\Delta A = 2B\Delta a$. Recently, Neimitz et al. [11] tried to calculate the increment $\Delta J_{(i)}^{\mathrm{pl}}$ via the total differential of eq. (10). They overlooked however, that the latter consists of two parts, namely for constant displacement and for constant crack length,

$$dJ^{\mathrm{pl}} = \left( \frac{\partial J^{\mathrm{pl}}}{\partial a} \right)_{V^{\mathrm{pl}}} da + \left( \frac{\partial J^{\mathrm{pl}}}{\partial V^{\mathrm{pl}}} \right)_{a} dV^{\mathrm{pl}}. \tag{14}$$

The second part of eq. (13) is missing in the authors' calculation. In addition, the discretisation of the differentials is not properly performed, bearing in mind that $\Delta f_{(i)} = f_{(i)} - f_{(i-1)} = f'(\bar{x})\Delta x_{(i)}$ with $x_{(i-1)} < \bar{x} < x_{(i)}$. The derivation of eq. (11) by means of the total differential of eq. (10) is elaborate [12], however, and is not presented here.

Other authors apply ASTM E 561 [2] for large thin panels as used in the aircraft industry, e.g. Schwalbe and Setz [13], Reynolds [14], Haynes and Gangloff [15].

## Validation of the R-curve Formulas

### Tests and Numerical Models.

Investigating the accuracy of the various equations for evaluating $J$ requires reference solutions to compare with. This is only possible by applying numerical models accounting for crack extension, which provides consistent data for the quantities used in the above equations, namely $F$, $V$ and $a$, as well as for the $J$-integral. As has been shown in several papers, e.g. [16], [17], [18], [19], ductile crack extension in metal sheets can be adequately modeled with cohesive elements. The data presented here have been obtained for an aluminium-magnesium alloy Al 5083 H321, $E$ = 71600 MPa, $R_{\mathrm{p0.2}}$ = 240 MPa, which is widely used in shipbuilding and automotive industry. Several fracture specimens with different sizes have been manufactured from rolled plates of 3 mm thickness, which were tested under quasi-static conditions. The parameters of the cohesive model, namely the cohesive strength, $\sigma_{\mathrm{c}}$ = 560 MPa, and the separation energy, $\Gamma_{\mathrm{c}}$ = 10 kJm$^{-2}$, have been determined from C(T) specimens of $W$ = 50 mm; for details see [17]. Figs 1a,b show the experimental and numerical force vs. displacement curves of C(T) and M(T) specimens of width $W$ = 50 mm and Figs 1c,d of C(T) and M(T) specimens of width $W$ = 150 mm. The coincidence

between test and simulation results is reasonable, keeping in mind that a unique set of cohesive parameters has been used to model crack extension in various specimen geometries and sizes. Maximum force is overestimated by 6.5% for the C(T) 150, Fig 1c, which is the largest deviation from test results, which differ by 3% among themselves. Any discrepancies occurring between test and simulation data would not affect the following conclusions, anyway, as the intention is just to have a set of consistent data to check the accuracy of the above *J* formulas.

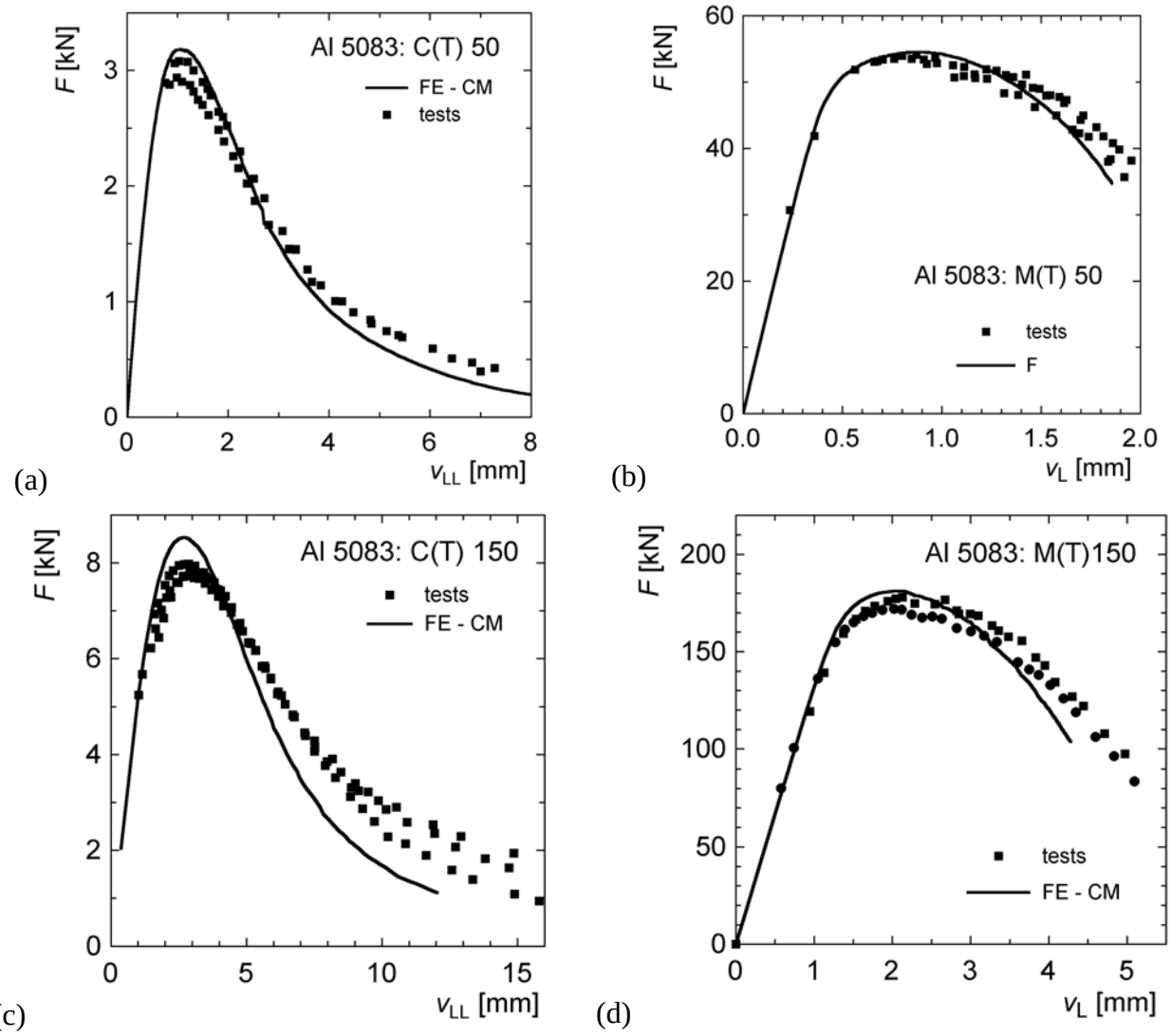


Fig. 1: Force-displacement curves of 3 mm thick, cracked panels, comparison of tests and simulations with the cohesive model; (a) C(T) $W$ = 50 mm, $a_0$ = 25 mm, (b) M(T) $W$ = 50 mm, $a_0$ = 15 mm, (c) $W$ = 150 mm, $a_0$ = 75 mm, (d) M(T) $W$ = 150 mm, $a_0$ = 30 mm.

As the controversial discussion on constraint dependence of cohesive parameters is everlasting and sometimes conducted grimly, some comments appear necessary at this point though the problem is not a principal issue of the present paper. There is no doubt, that generally cohesive parameters are constraint, i.e. geometry dependent. This does not mean however that any transfer of the parameters from one specimen configuration to another is improper. There is plenty of evidence that a unique set of cohesive parameters yield reasonable results for various geometries [16], [17], [18], [24]. The reasons are simple:

i. Possible differences in constraint for plane stress conditions are generally small.

ii. The contribution of the local separation energy to the overall dissipated energy, and hence to a $J_R$-curve is negligibly small, as has been shown in other investigations [24] and will also be substantiated later in the present paper.

After all, the transferability and hence the predictive capabilities of the cohesive model with constraint independent parameters are much better than those of $J_R$- and $\delta_R$-curves, as will also be proven in the following.

**Evaluation of Numerical Data**

The data of the numerical simulations are taken to evaluate $J_R$-curves. The $J$-integral value calculated by ABAQUS is used as reference. Special care has to be taken to ensure obtaining a "far-field" value of $J$ [20], which is comparable to the values calculated from a global force-displacement curve. Fig 2 shows the results. The abscissa is scaled in both absolute and normalised values of crack extension.

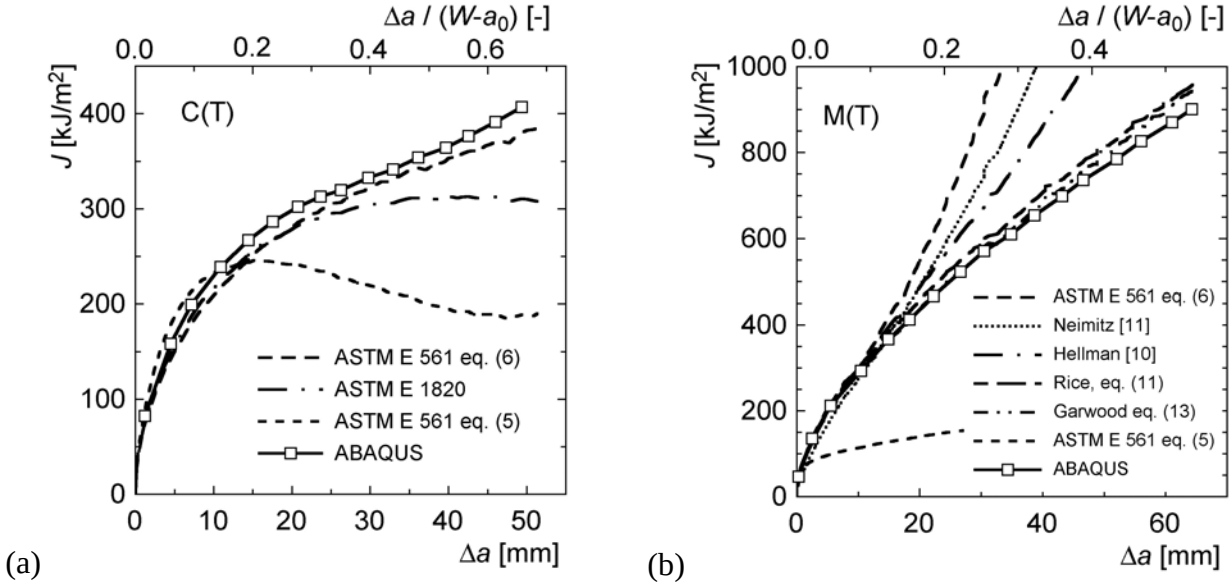


Fig. 2: $J_R$-curves of cracked panels of Al 5083, thickness 3mm, width 150 mm, comparison of various evaluation procedures; (a) C(T), (b) M(T)

Generally, little differences occur up to crack extensions of $\Delta a \le 10\,\text{mm}$, which is $0.13(W-a_0)$ for the C(T) and $0.08(W-a_0)$ for the M(T), respectively, but the deviations may become significant for large crack growth. ASTM E 561 based on the plastic zone correction, eq. (5), fails beyond $\Delta a > 10\,\text{mm}$ for the C(T) and even shows a decreasing $J_R$-curve for large crack extension, which is physically meaningless. ASTM E 1820 becoming improper beyond $\Delta a > 0.27(W-a_0)$. An analysis of the data revealed a discrepancy between the FE data and the ASTM E 1820 procedure in splitting elastic and plastic energies. Whereas ASTM E 561 based on the compliance, eq. (6), gives the best approximation up to $\Delta a = 50\,\text{mm} = 0.66(W-a_0)$ for the C(T), it overestimates $J$ significantly beyond $\Delta a > 0.12(W-a_0)$ for the M(T), and based on the plastic zone correction, eq. (5), it does not produce any useful result at all. This is even more critical as this standard is particularly used for centre-cracked panels [12], [14], [15]. The formula of Neimitz et al. [11] starts overestimating $J$ beyond $\Delta a > 0.17(W-a_0)$. Eq. (11) according to Rice et al. [5] and eq. (13) according to Garwood et al. [9] produce perfect approximations for the M(T) up to $\Delta a = 65\,\text{mm} = 0.54(W-a_0)$.

**Significance of R-curves**

Once a correct R-curve can be generated from the experimental data, the question of its significance for describing ductile crack extension may be raised, often addressed as "validity". No respective recommendations or guidelines are provided in the standards. This question cannot be generally answered here, as this would require systematic experimental and numerical investigations. The present data may be used however to give a first impression.

R-curves or C(T) and M(T) are presented in Fig. 3 in terms of both $J$ and CTOD, where the latter is defined as $\delta_5$ according to Schwalbe [21]. Test and simulation results are displayed.

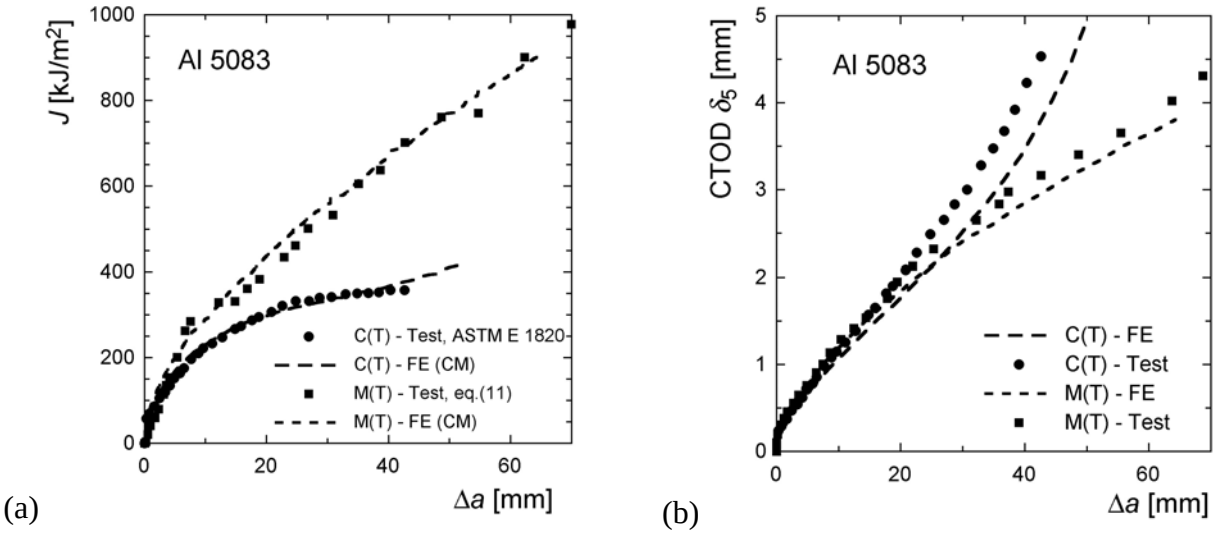


Fig. 3: R-curves of 3 mm thick C(T) and M(T) specimens of Al 5083, width 150 mm, as obtained from tests and simulations with the cohesive model; (a) $J$-integral, (b) CTOD $\delta_5$

The range of validity, i.e. of geometry independence is obviously much larger for the CTOD R-curves. This finding, which is much older [10] than the numerical analyses of tests presented here, gave rise for establishing ASTM E 2472 [3] as a standard on “resistance to stable crack extension under low-constraint conditions”. It covers the measurement of $\delta_5(\Delta a)$ curves and the crack-tip opening angle CTOA as fracture parameters [22]. CTOA can be determined optically or via $\delta_5(\Delta a)$ curves [23]. Measurements and simulations of crack extension based on CTOA [17] showed that it is to some extent geometry-independent, i.e. independent on the specimen size and the type of loading (uni- and biaxial tension, bending), but it will depend on the specimen thickness and is primarily suited for thin panels. Different from the cohesive model, it cannot be used to model crack kinking or branching [19].

With regard to the general discussions on constraint dependence, Fig 3 demonstrates that the predictive capabilities of simulations with a unique set of cohesive parameters are much better than those of $J_R$- and $\delta_R$-curves. Whereas the latter become geometry dependent sooner or later after some crack extension, $\Delta a$, the cohesive model captures the geometry dependence over the whole measured range.

## Energy Balance at Crack Extension

### Total Energy

Beside the validation of R-curve formulas, the numerical simulations allow for an analysis of data which is not accessible in the experiments but will improve the understanding of the mechanical processes at crack extension. For this purpose, the energy balance is of primary concern. The work of external forces, $W^{\mathrm{ex}}$, equals the internal energy consisting of the stored (recoverable) elastic energy, $U^{\mathrm{el}}$, the (non-recoverable) global plastic strain energy, $U^{\mathrm{pl}}$, and the local separation energy, $U^{\mathrm{sep}}$,

$$W^{\mathrm{ex}} = \int F \,\mathrm{d}V = U^{\mathrm{el}} + U^{\mathrm{pl}} + U^{\mathrm{sep}} \ . \tag{14}$$

The latter results from the material separation in the process zone ahead of the crack tip, which is modelled by cohesive elements [24], [25] following a decohesion or traction-separation law, $\sigma_{\mathrm{n}}(\delta_{\mathrm{n}})$,

$$U^{\mathrm{sep}} = \Gamma_{\mathrm{c}} B \Delta a = B \int_{a_0}^{a_0+\Delta a} \left( \int_0^{\delta_{\mathrm{c}}} \sigma_{\mathrm{n}} \,\mathrm{d}\delta_{\mathrm{n}} \right) \mathrm{d}a \ . \tag{15}$$

Fig. 4 displays the respective portions of $W^{\mathrm{ex}}$, in the course of crack extension. The plastic strain energy, $U^{\mathrm{pl}}$, starts exceeding the elastic energy, $U^{\mathrm{el}}$, at $\Delta a \geq 0.09\left(W - a_0\right)$ in the C(T) and at $\Delta a \geq 0.19\left(W - a_0\right)$ in the M(T) specimen. This means, that elastic deformation dominates total deformation over a longer range of crack extension in the M(T), which is characteristic for a tensile type specimen in contrast to a bend type specimen. For $\Delta a > 0.5\left(W - a_0\right)$ more than 90% of external work in the C(T) and more than 80% of external work in the M(T) are spent by plastic deformation.

In addition, Fig 4 allows for a quantification of the range of application expressed in ASTM E 561, "so long as specimens are of sufficient size to remain predominantly elastic throughout the duration of the test". Quantifying this qualitative statement as $U^{\mathrm{el}} \geq 0.8\, W^{\mathrm{ex}}$, or any other reasonable number, the application limits of ASTM E 561 would be $\Delta a \leq 1\mathrm{mm}$ for the C(T) and $\Delta a \leq 4\mathrm{mm}$ for the M(T). Note of course, that these numbers refer to the present specimen dimensions and may be different for others. They indicate, however, that the application of ASTM E 561 can be quite limited. In this respect, the good coincidence of the $J_{\mathrm{eff}}$-curve of the C(T) as calculated from the compliance with the reference R-curve in Fig. 3a even for large crack extension is surprising. A qualitative statement requiring a “sufficient size” is not at all helpful in a standard, however.

Finally, Fig. 4 confirms what has been found in other investigations [24], that the local separation energy, $U^{\mathrm{sep}}$, in ductile tearing is negligibly small compared to the remote work of plastic deformation, $U^{\mathrm{pl}}$. For $\Delta a = 0.5\left(W - a_0\right)$ $U^{\mathrm{sep}}$ is 3% of $U^{\mathrm{pl}}$ in the C(T) and 0.4% in the M(T), which makes it hardly visible in Fig. 4b. What is measured as $U^{\mathrm{pl}}$ in R-curve testing is hence only to a minor part the actual work of separation in the process zone. Just the numerical model allows for

separating these two fractions of dissipated energy. On the other hand, these results put detached discussions on the constraint dependence of cohesive parameters into perspective.

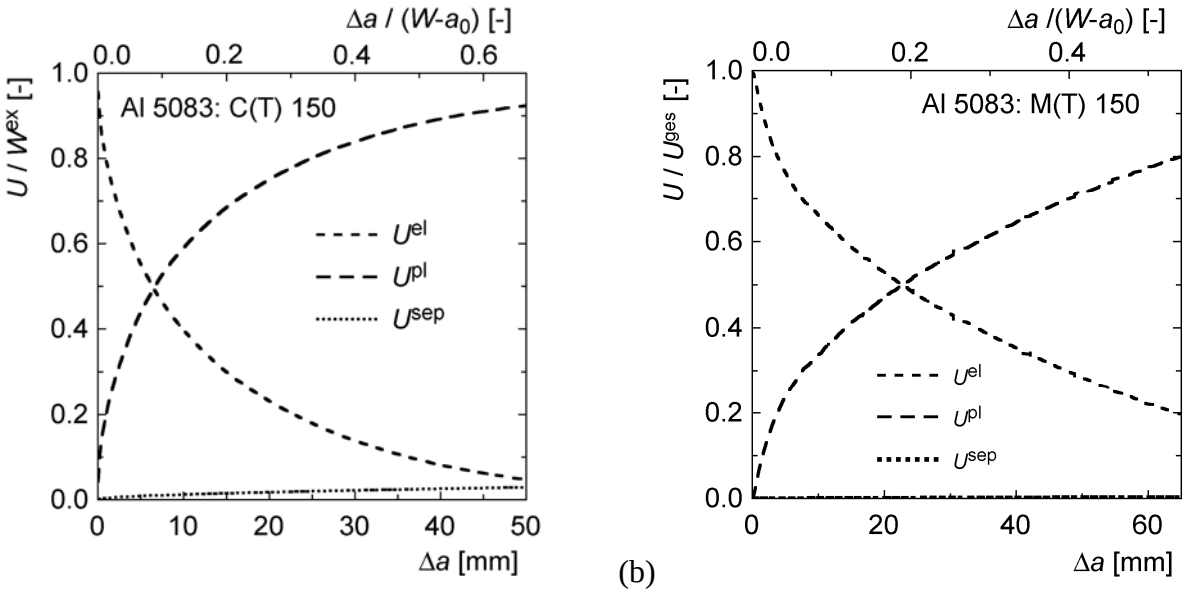


(a) (b)

Fig. 4: Recoverable and non-recoverable portions of the work of external forces; (a) C(T), (b) M(T)

**Dissipation Rates**

In a fundamental criticism of the toughness concept of elastic-plastic fracture mechanics, Turner [26] stated, that the cumulative quantity $J$ is not the crack-driving force of crack extension in Griffith's sense any more. Instead, he proposed to define crack growth resistance in terms of the dissipation rate,

$$R^{\mathrm{dis}} = \frac{\mathrm{d}U^{\mathrm{pl}}}{\mathrm{d}A} + \frac{\mathrm{d}U^{\mathrm{sep}}}{\mathrm{d}A} = \frac{\mathrm{d}U^{\mathrm{pl}}}{\mathrm{d}A} + \Gamma_{\mathrm{c}} = \frac{\mathrm{d}W^{\mathrm{ex}}}{\mathrm{d}A} - \frac{\mathrm{d}U^{\mathrm{el}}}{\mathrm{d}A} \ , \tag{16}$$

where $A$ is the crack area as above in eq. (1). This definition is a straightforward transfer of Griffith's elastic energy release rate to elastic-plastic changes of state [25], which is compatible with incremental theory of plasticity. Different from $J$, $R^{\mathrm{dis}}$ decreases with crack extension. It is not a material characteristic but a structural quantity like $J$, as it includes remote plastic work. Several authors [27], [28], [29], [30] have adopted this concept and demonstrated its potential, since. One of the striking features of $R^{\mathrm{dis}}(\Delta a)$ is, that it follows a universal representation by a decreasing exponential curve,

$$R^{\mathrm{dis}}(\Delta a) = R_{\infty}^{\mathrm{dis}} \left[ 1 + \left( \frac{R_0^{\mathrm{dis}} - R_{\infty}^{\mathrm{dis}}}{R_{\infty}^{\mathrm{dis}}} \right) \exp\left( -\lambda \frac{\Delta a}{W} \right) \right] \ , \tag{17}$$

which starts at some initial value, $R_0^{\mathrm{dis}}$, and reaches a saturation value, $R_{\infty}^{\mathrm{dis}}$, the so-called crack-propagation energy rate, for stationary crack growth [27]. The parameter $\lambda$ controls the intensity of

decline from $R_0^{\mathrm{dis}}$ to $R_\infty^{\mathrm{dis}}$. These three parameters together with the initiation toughness, $J_\mathrm{i}$, characterise the ductile tearing resistance of a specimen [31].

The evaluation of the numerical simulations in Fig. 5 confirms these characteristics of $R^{\mathrm{dis}}$. Whereas $\Gamma_\mathrm{c}$ is a constant according to the cohesive model, $\mathrm{d}U^{\mathrm{pl}}/\mathrm{d}A$ decreases monotonically to some saturation value. The numerical differentiation of the numerical data produces oscillations, which have been smoothed by a fit curve according to eq. (17). The respective parameter values are summarised in Table 1. The difference between $R^{\mathrm{dis}}$ and $\mathrm{d}U^{\mathrm{pl}}/\mathrm{d}A$ is just a constant, $\Gamma_\mathrm{c}$, affecting $R_\infty$.

| | $R_0^{\mathrm{dis}}$ [kJ/m$^2$] | $R_\infty^{\mathrm{dis}}$ [kJ/m$^2$] | $\lambda$ [-] |
|---|---|---|---|
| C(T) | 548 | 140 | 5.66 |
| M(T) | 3443 | 760 | 11.1 |

Table 1: Parameters characterising tearing resistance in terms of dissipation rate, $R^{\mathrm{dis}}$, according to eq. (17)

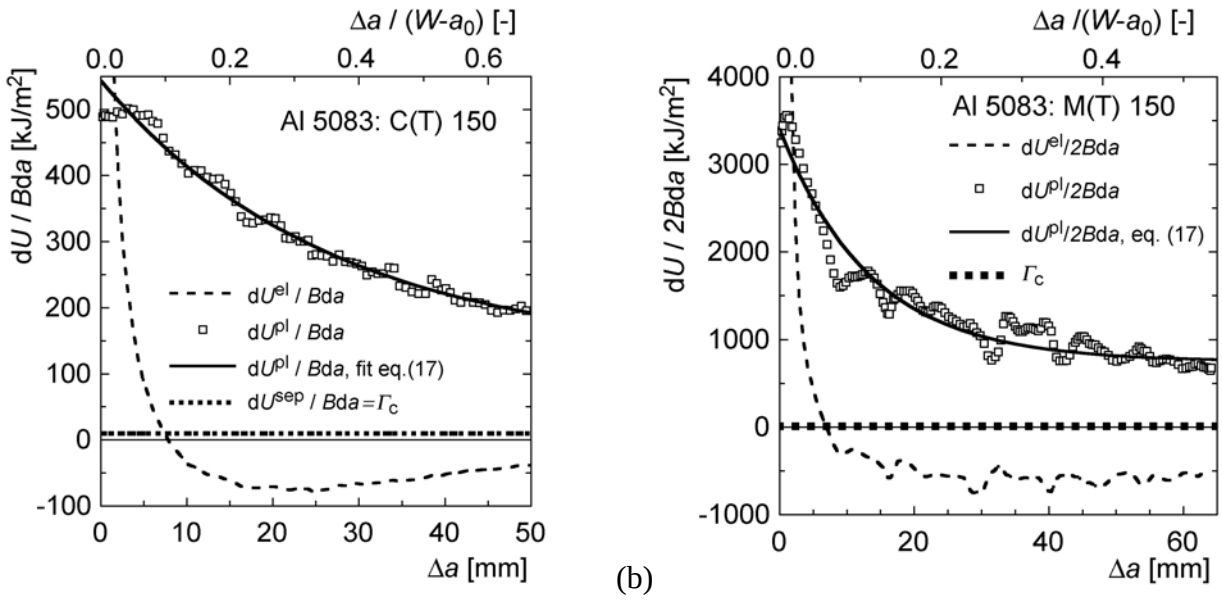


Fig. 5: Energy rates at crack extension, (a) C(T), (b) M(T)

Fig. 5 and Table 1 substantiate the following conclusions on the differences between the two specimen types C(T) and M(T) with respect to the energy dissipation rate at crack extension. The specific numbers refer to the dimensions of the investigated specimens, of course, but the qualitative trend is general:

- Stationary crack extension is reached much later in the C(T) than in the M(T), $\lambda^{\mathrm{CT}}/\lambda^{\mathrm{MT}} = 0.51$.
- The dissipation rate in the M(T) is significantly higher than in the C(T), $R_0^{\mathrm{dis(MT)}}/R_0^{\mathrm{dis(CT)}} = 6.3$, $R_\infty^{\mathrm{dis(MT)}}/R_\infty^{\mathrm{dis(CT)}} = 5.4$.

- The local separation energy contributes nearly negligibly to the global dissipation rate, $\Gamma_c / R_0^{\mathrm{dis(CT)}} = 1.8\%$, $\Gamma_c / R_\infty^{\mathrm{dis(CT)}} = 7.1\%$, $\Gamma_c / R_0^{\mathrm{dis(MT)}} = 0.3\%$, $\Gamma_c / R_\infty^{\mathrm{dis(MT)}} = 1.3\%$, but nevertheless controls the process of crack extension. This is a justification of taking $\Gamma_c$ as a material parameter in the simulations, though it is unquestionably constraint dependent [24], [25].

## Summary and Conclusions

There is a need, particularly in the aircraft industry, to adopt fracture mechanics concepts like R-curves for ductile crack extension to thin-walled panels and shells under conditions, which are close to plane stress. Respective test procedures and standards are not as well founded as those for plane-strain specimens or do not even exist at all. Though the basic concepts for determining $J$ from experimental force-displacement records are quite old, they have not yet found their way into standards or guidelines for other than thick bend-type specimens. This has been the motivation for validating various $J$ formulas existing in the standards and in the literature by means of numerical simulations of large crack extension in thin C(T) and M(T) specimens.

ASTM E 1820 has a limited range of application for C(T)-type specimens of $\Delta a_{\max} \le 0.25(W - a_0)$. It does not provide any support for M(T)-type specimens. The given validity conditions with respect to the specimen thickness concern the application of the R-curves to plane-strain conditions, but not the accuracy of the $J$ formulas.

The $K_R$-curve concept of ASTM E 561, which is specifically dedicated to panels without thickness requirements, is accepted for structural assessment in the aerospace industry, but its background is obsolete. It might work well in some cases but completely fail in others, and it does not provide any window of application. Two options for determining the “effective” crack length are provided which yield totally different results. The option of a plastic zone correction is virtually useless. The alternate option of determining $a_{\mathrm{eff}}$ from the specimen compliance worked even better than the ASTM E 1820 procedure for the C(T), but with the experimental techniques of present days given, there is no real necessity of defining an "effective" crack length.

$J_R$-curves of thin M(T) specimens can be accurately determined up to large crack extensions by the formulas derived according to Rice et al. [5], eq. (11), or Garwood et al. [9], eq. (13). There is no need for other formulas or empirical equations, whose validity range is limited.

The range of transferability is much larger for CTOD than for $J$ based R-curves. This would favour the future practical application of ASTM E 2472 as a standard dedicated to measure the resistance to stable crack extension under low-constraint conditions based upon $\delta_5(\Delta a)$ curves and the crack-tip opening angle. The CTOA is particularly useful for describing stationary crack extension, where it was found to be constant. It is to some extent geometry-independent, i.e. independent on the specimen size and the type of loading (uni- and biaxial tension, bending).

Cohesive models as applied in the present investigation are the most versatile tools for modelling crack extension and predicting the residual strength of cracked panels and shells. However, no rules or guidelines for their application and parameter identification exist yet.

The concept of the dissipation rate at crack extension is favoured by several authors and has been used to formulate stability conditions [29] in an extended sense of Griffith's condition. The present numerical study presents values of the dissipation rate in thin panels for the first time, indicating that features known from "plane-strain" specimens [31] also hold for "plane-stress" specimens. Like CTOA, the dissipation rate approaches a stationary value. It helps understanding effects of geometry dependence of R-curves but is still far from being used as fracture criterion.

**References**


[1] ASTM E 1820-06: Standard test method for measurement of fracture toughness, Annual book of ASTM Standards, Vol 03.01, American Society for Testing and Materials, Philadelphia.

[2] ASTM E 561-05: Standard test method for K-R curve determination, Annual book of ASTM Standards, Vol 03.01, American Society for Testing and Materials, Philadelphia.

[3] ASTM E 2472-06: Standard test method for determination of resistance to stable crack extension under low-constraint conditions, Annual book of ASTM Standards, Vol 03.01, American Society for Testing and Materials, Philadelphia.

[4] Begley, J.A., Landes, J.D.: The *J*-integral as a fracture criterion. In: Fracture Toughness, ASTM STP 514 (1972), 1-23.

[5] Rice, J.R., Paris, P.C., Merkle, J.G.: Some further results of *J*-integral analysis and estimates. In: Progress in Flaw Growth and Fracture Toughness Testing, ASTM STP 536 (1973), 231-245.

[6] Feddersen, R.E.: Discussion of the paper of 'Plane strain crack toughness testing of high strength metallic materials' by W.F. Brown, Jr. and J.E. Srawley. In: ASTM STP 410 (1966), 77-79.

[7] Eftis, J., Liebowitz, H.: On the modified Westergaard equation for certain plane crack problems. Int J. Fracture Mechanics 8 (1972), 383-392.

[8] Tada, H., Paris, P.C., Irwin, G.R.: The Stress Analysis of Cracks Handbook, American Society of Mechanical Engineers (ASME), ASME Press, New York, 2000.

[9] Garwood, S.J., Robinson, J.N., Turner, C.E.: The measurement of crack growth resistance curves (R-curves) using the *J* integral. Int. J. Fracture 11 (1975), 528-530.

[10] Hellmann, D., Schwalbe, K.-H.: Geometry and size effects on *J*-R and $\delta$-R curves under plane stress conditions. In: Fracture Mechanics: 15th Symp. ASTM STP 833 (1984), 577-605.

[11] Neimitz, A., Dzioba, I., Galkiewicz, G., Molasy, R.: A study of stable crack growth using experimental methods, finite elements and fractography. Engng. Fract. Mech. 71 (2004), 1325-1355.

[12] Brocks, W., Anuschewski, P.: Risswiderstandskurven von Blechen. Technical Note GKSS/WMS/08/06, Institute of Materials Research, GKSS Research Centre, Geesthacht, 2008.

[13] Schwalbe, K.-H., Setz, W.: R curve and fracture toughness of thin sheet materials. J. Testing and Evaluation 9 (1981), 182-194.

[14] Reynolds, A.P.: Comparison of R-curve methodologies for ranking the toughness of aluminum alloys. J. Testing and Evaluation 24 (1996), 406-410.

[15] Haynes, M.J., Gangloff, R.P.: High resolution R-curve characterisation of the fracture toughness of thin sheet aluminium alloys. J. Testing and Evaluation 25 (1997), 82-98.

[16] Scheider, I., Brocks, W.: Cohesive elements for thin-walled structures. Comp. Mater. Sci. 37 (2006), 101-109.

[17] Scheider, I., Schödel, M., Brocks, W., Schönfeld, W.: Crack propagation analyses with CTOA and cohesive model: Comparison and experimental validation. Engng Fract. Mech 73 (2006), 252-263.

[18] Brocks, W., Scheider I., Schödel, M.: Simulation of crack extension in shell structures and prediction of residual strength. Arch. Appl. Mech. 76 (2006), 655-665.

[19] Brocks, W., Scheider, I.: Prediction of crack path bifurcation under quasi-static loading by the cohesive model. Structural Durability & Health Monitoring 3 (2007), 69-79.

[20] Brocks, W., Scheider, I.: Reliable *J*-values - Numerical aspects of the path-dependence of the *J*-integral in incremental plasticity. Materialprüfung. 45 (2003), 264-275.

[21] Schwalbe, K.-H.: Introduction of $\delta_5$ as an operational definition of the CTOD and its practical use. In: ASTM STP 1256 (1995), 763-78.

[22] Newman, J.C., James, M.A., Zerbst, U.: A review of the CTOA/CTOD fracture criterion. Engng. Fract. Mech. 70 (2003), 371-385.

[23] Heerens, J., Schödel, M.: On the determination of the crack tip opening angle, CTOA, using light microscopy and $\delta_5$ measurement technique. Engng. Fract. Mech. 70 (2003), 417-426.

[24] Siegmund, T., Brocks, W.: Prediction of the work of separation and implications to modeling. Int. J. Fracture 99 (1999), 97-116.

[25] Brocks, W.: Cohesive strength and separation energy as characteristic parameters of fracture toughness and their relation to micromechanics, Structural Integrity and Durability 1 (2005), 233-243.

[26] Turner, C.E.: A re-assessment of ductile tearing resistance, Part I: The geometry dependence of J-R curves in fully plastic bending, Part II: Energy dissipation rate and associated R-curves on normalized axes, Fracture Behaviour and Design of Materials and Structures, Preprints 8th European Conf. on Fracture (ed. D. Firrao), Turin 1990, Vol. II, Engineering Mechanics Advisory Services, Warley (1990), 933-949, 951-968.

[27] Memhard, D., Brocks, W., Fricke, S.: Characterization of ductile tearing resistance by energy dissipation rate. Fatigue Fract. Engng. Mater. Struct. 16 (1993), 1109-1124.

[28] Turner, C. E., Kolednik, O.: Application of energy dissipation rate arguments to stable crack growth. Fatigue Fract. Engng Mater. Struct. 20 (1994), 1109-1127.

[29] Sumpter, J.D.G.: An alternative view of R curve testing. Engng. Fract. Mech. 64 (1999), 161-176.

[30] Sumpter, J.D.G.: Energy rates and crack stability in small scale yielding. Int. J. Fracture 130 (2004), 667-681.

[31] Brocks, W., Anuschewski, P.: Parametrizing ductile tearing resistance by four parameters. Engng. Fract. Mech. 71 (2004), 127-146.